

COMMISSIONING THE GTA ACCELERATOR*

O. R. Sander, W. H. Atkins, G. O. Bolme, S. Bowling, S. Brown, R. Cole, R. Connolly,^{††}
 J. D. Gilpatrick, R. Garnett, F. W. Guy, W. B. Ingalls, K. F. Johnson, D. Kerstiens, C. Little, R. A. Lohsen, S. Lloyd,
 W. P. Lysenko, C. T. Mottershead, G. Neuschaefer, J. Power, D. P. Rusthoi, K. Saadatmand,[†]
 D. P. Sandoval, R. R. Stevens, Jr., G. Vaughn, E. A. Wadlinger,
 R. Weiss,^{††} and V. Yuan

Los Alamos National Laboratory
 P.O. Box 1663, MS H818, Los Alamos, NM 87545

Introduction

The Ground Test Accelerator (GTA) is supported by the Strategic Defense Command as part of their Neutral Particle Beam (NPB) program. Neutral particles have the advantage that in space they are unaffected by the earth's magnetic field and travel in straight lines unless they enter the earth's atmosphere and become charged by stripping. Heavy particles are difficult to stop and can probe the interior of space vehicles; hence, NPB can function as a discriminator between warheads and decoys. We are using GTA to resolve the physics and engineering issues related to accelerating, focusing, and steering a high-brightness, high-current H⁻ beam and then neutralizing it. Our immediate goal is to produce a 24-MeV, 50-mA device with a 2% duty factor.

Description of GTA

The GTA design consists of a H⁻ injector, a radio-frequency quadrupole (RFQ), a drift-tube linac (DTL) and an output optics section (Fig. 1). The characteristics of the H⁻ injector are given in Table 1. Figure 2 is a schematic of the injector.

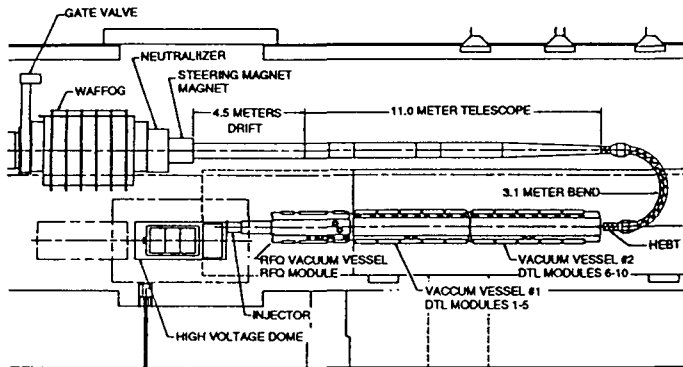


Fig. 1. Schematic of the GTA.

Between the RFQ and the DTL we have placed an intertank matching section (IMS) whose functions are to match and steer the beam from the RFQ to the DTL. Table 3 gives the characteristics of the IMS. Figure 3 is a schematic of the IMS.

*Work supported and funded by the US Department of Defense, Army Strategic Defense Command, under the auspices of the US Department of Energy.

[†] Industrial partner, Grumman Corporate Research Center

^{††} Industrial partner, Grumman Space and Electronics Division

Table 1
 Injector Characteristics

Source type	Cesiated surface plasma source (SPS)
Peak source current	56 mA
Output energy	35 keV
Length	0.7 m
Focusing	two solenoids
Steering	Two Lambertson magnets
Diagnostics	Beam emittance and current

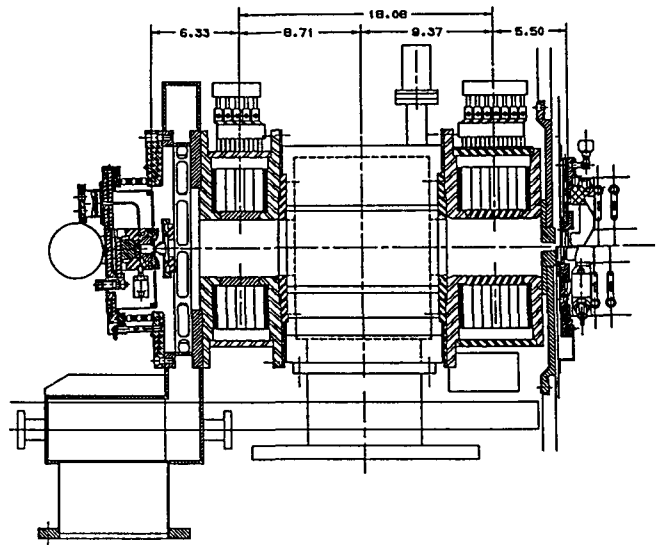


Fig. 2. Schematic of the injector.

The characteristics of the RFQ are given in Table 2

Table 2
 RFQ Characteristics

Type	four vane
Material	Aluminum coated with copper
Input/output energy	35 keV/ 2.5 MeV
Length	2.8 m
Vane voltage	56 kV
Peak field	36 MV/m (1.8 Kilpatrick)
Frequency	425 MHz
Final modulation	2.17
Radius	2.09 to 2.91 mm
Tuning	35 static and 8 controllable slug tuners
Unloaded Q	25000 at 20-35K
Q enhancement	3.2
Number of cells	250
Position adjustment	± 1 mm

Table 3
 IMS Characteristics

Transverse focusing	Four variable field quadrupoles (VFQ)
Magnet material	Samarium cobalt
Longitudinal focusing	Two 425-MHz bunchers (copper)
Buncher unloaded Q	56000
Q enhancement	5.1
Steering	Two movable fixed field permanent magnet quadrupoles (PMQ)
Diagnostics	Beam centroids, current and profile

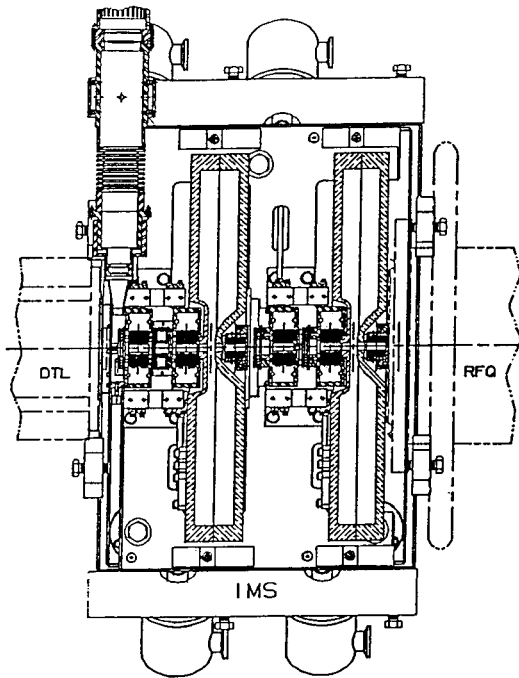


Fig. 3. Schematic of the IMS.

Table 4 gives the DTL characteristics.

 Table 4
 DTL Characteristics

Number of modules	10
Final output energy	24.2 MeV
Material	Copper
Focusing	Samarium cobalt PMQs
E_0T	Ramped, 1.25 to 5.8 MV/m
Frequency	850 MHz
Frequency tuning	Two controllable paddle tuners/module
Position adjustment	± 5 mm
Q	44000
Q enhancement	3.4

The DTL was divided into 10 modules for ease of fabrication and drift-tube magnet alignment.

The output optics begins with a matching and steering section, the high energy beam transport (HEBT). As in the IMS, it contains four VFQs and two fixed-field moveable PMQs. The following beam transport section bends the beam by 180 degrees; its purpose is to shorten GTA. A momentum compactor reduces the momentum spread of the

beam and reduces the chromatic aberrations in the following expending telescope. We built the telescope objective lens with a large, 1-m bore to increase beam on target. The telescope is designed to correct up to fifth-order aberrations. Its gradient length product is 0.04 T, which can be increased to 0.08 T for 100-MeV operation. Beam steering is accomplished with a modified cosine-wound magnet whose field-length product is 0.008 Tm. The steering range is 1.25 degrees. The final beam neutralization will be done using a carbon foil with a stripping fraction of 55 percent. Output beam diagnostics consists of pinhole plates to measure the full four-dimensional emittance and WAFFOG [1] (Wire And Fluorescent Fiber Offset Grid sensing technique), which gives the y, x, x' and x, y, y' distributions.

We designed all rf linac structures for cw operation with LH₂ cooling. We chose copper construction on the DTLs, rather than the lighter aluminum, because of copper's higher thermal conductivity. For safety reasons we are cooling with gaseous helium and limit operation to 2% duty factor. Cryogenic operation offers two advantages. The rf cavities are very mechanically stable during the transition from standby to full-power operation, and the total rf power requirement is reduced. For the present commissioning and off-line rf cavity characterization, we are using two 750-W refrigerators. For the commissioning of the 24-MeV DTL, we will use our 40-kW cryo-plant that was recently commissioned and accepted.

Cryogenic operation presents unique challenges. Remote position sensing is required because the rf structures must be inside a vacuum vessel. Radio frequency interference (RFI) leakage from the rf structures must be suppressed by installing waveguide cut-off tubes on the pump-out ports. RFI shielding is required on beam diagnostics. Effects of thermal contraction must be taken into account in the alignment procedures. Thermal barriers are required on the structure mounts, rf drive lines, and rf resonance tuners. Special copper-to-steel and aluminum-to-steel joints are required to withstand the high pressures and low temperatures.

Diagnostics, Control and RF Power Systems

Beam diagnostics are installed to measure the beam longitudinal and transverse centroids and emittances. A portable diagnostics plate (D-plate) measures the beam characteristics as successive accelerator components are added. The transverse and longitudinal emittances are measured using the standard slit-collector method and LINDA [2], respectively. Beam position, energy, and phase are measured using microstrip beam position monitors (BPMs). Beam current is measured with current toroids and Faraday cups. BPMs are also placed in the IMS and on each DTL module. A video profile monitor measures the beam transverse profiles in the IMS by digitizing the visible light from beam-gas interactions. Diagnostics also measure the temperature, position, magnetic field, vacuum levels, and gap voltages of the GTA components.

The GTA control system is the AT-division experimental physics and industrial control system, (EPICS). It is based on a VME bus using distributed input-output controllers (IOCs) that communicate over Ethernet. Individual IOCs control the injector, rf power, component

positions, beam steering and focusing, diagnostics, vacuum controls, and accelerator interlocks. Synchronous data are obtained and archived [3] by time-stamping data using synchronized IOC clocks [4]. The archived data can be exported for further analysis and display on Macintosh computers. Typically, we collect 100 channels of synchronous data at 5 Hz. During normal operations we will use up to six Open-Windows, version II control screens on each of our SUN-SPARC work stations. Allen-Bradley modules are used extensively.

The rf system uses in-phase and quadrature (I&Q) control [5]. Because most simulations and predictions use phase and amplitude as variables, the rf control system screen presents phase and amplitude to the experimenter. The conversion to I&Q is transparent to the experimenter. Burle 4616 tetrodes are the high-power amplifiers for the RFQ and IMS rf cavities; the Thompson TH2138A klystrons power the DTL modules.

Commissioning Plan

The GTA commissioning schedule is shown in Table 5.

Table 5
Commissioning Schedule

Experiment Notation	Accelerator Component tested	Status
1A with long LEBT	Injector	Completed 9/90
1A with short LEBT	Injector	Completed 5/91
1B	RFQ	Completed 6/91
1C	IMS	Completed 4/92
2A	DTL #1	9/92
2B	DTL 1-5 (2- $\beta\lambda$ -DTLs)	FY 93
2D	DTL 1-10 (2 & 1 $\beta\lambda$ -DTLs)	FY 94
3	HEBT, Bend, Telescope	FY 95

RF Cavity Construction, Conditioning and Characterization

Using bead-pull equipment, which we modified for cryogenic operation, we established the desired RFQ quadrupole fields at room temperature and verified that these fields remained constant to $\leq 1\%$ at 20 K. The dipole fields are only 2-3% of the quadrupole field. The RFQ structure is very stable. Three DTL modules have been characterized. The DTL fields remained stable to $\pm 0.5\%$ when the modules were cooled to 20 K. Using the taut wire technique [6], which we modified for cryogenic operation, we aligned the drift tube PMQs to ± 1 -mil tolerances at room temperature and determined that the PMQs remained within the ± 2 -mil specification after the DTL modules were cooled to 20 K. All cavities were mounted with thermal barriers; heat losses to the cavities were consistent with calculations.

Initial conditioning of the RFQ and DTL modules at cryogenic temperatures was straightforward and typically took 2-3 hours to reach design power levels. The IMS cavities were more difficult to condition because of low-power multipactoring and required switching to cw conditioning from our usual 5-Hz pulsed mode. The RFQ is

reconditioned immediately each morning after 8 to 10 hours of no activity. During installation periods the RFQ has frequently been exposed to air for month-long periods; reconditioning times have not been longer than half an hour. Under similar conditions the IMS and DTL structures require 2-3 hours to recondition. REXOLITE[®] rf vacuum windows have shown no evidence of breakdown; however, we were required to machine 1/8-in. ridges on the inner and outer radii of the RFQ window to prevent breakdown. Thermal breaks and local heaters are required on these drive lines.

Commissioning Results and Status

Experiment 1A

Initially we used a SPS [7] on GTA that was similar to that used on the accelerator test stand, (ATS). We found that by scaling the plasma region by four, we could obtain improved reliability and increased beam current. This scaled source is capable of 2% duty factor, and has operated at 1.5%. At a source current of 56 mA, typical currents at the RFQ entrance are 45 mA. We shorted our initial 1.3-m LEBT to 0.7-m in order to reduce H⁻ stripping losses and to reduce the emittance growth due to beam current fluctuations. With the shorter LEBT, we steer the beam using Lambertson dipoles that are centered inside the bore of the solenoid magnets. We find that the LEBT steering can be modeled in TRACE [8] by simply splitting each solenoid into two halves and inserting the angle deflection caused by the Lambertson dipoles. The solenoidal focusing gives us the ability to adjust the Courant-Snyder (CS) parameters around the predicted RFQ matched parameters (Fig. 4).

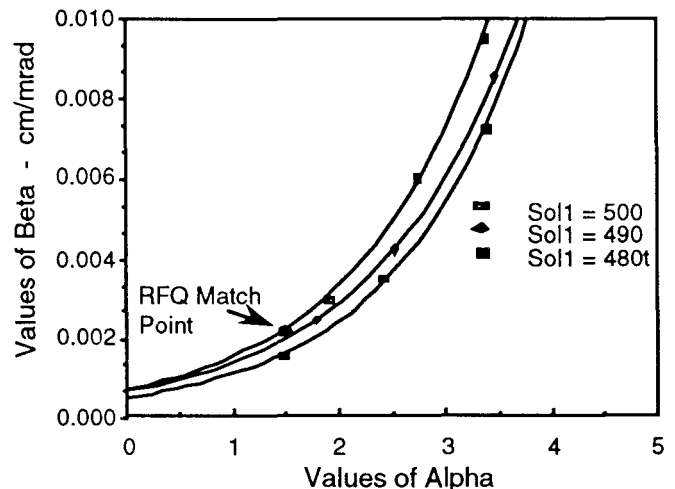


Fig. 4. The LEBT alpha vs. beta tuning diagram shows that variations in S1 and S2 can produce beams at and around the RFQ matched CS values.

Experiment 1B [9]

On our first attempt, the RFQ transmitted and accelerated beam. The best RFQ transmission was 72% with 32 mA accelerated. With lower input currents and smaller emittances, the transmission increased to 89% with 14 mA of accelerated beam. The alignment error of the

injector beam to the center of the RFQ acceptance was less than 8 mil. We determined that the best transmission occurred with LEPT focusing set to give the predicted RFQ-matched CS parameters. Figure 5 shows RFQ transmission versus solenoid settings. As expected, we found that the CS parameters of the RFQ output beam depend on the vane voltage (VV) or cavity power (P_{RFQ}). We measured the end-point energy of X-rays from the RFQ versus RFQ cavity power and determined that

$$VV = 7.11\sqrt{P_{RFQ}} \quad (1)$$

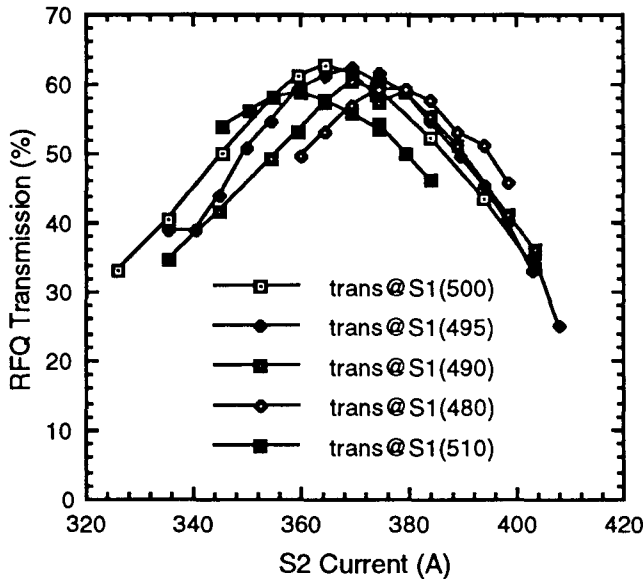


Fig. 5. RFQ transmission vs solenoid focusing. The solenoid currents S1 = 495A and S2 = 375 A, which give the maximum transmission, produce the CS parameters that equal the predicted RFQ matched values from simulations.

In Fig. 6 we show the mismatch factor [10] between the measured out beam CS parameters and the predicted parameters. The minimum mismatch factor occurs at 62 kW, which is the design RFQ cavity power. The RFQ transmission also depends on vane voltage. Figure 7 shows that the normalized measured transmission agrees with simulations in its dependence on vane voltage when we again choose 62 kW as the design cavity power. Repeated measurements of the RFQ output emittance are very similar and, when compared, have mismatch factors of ≤ 0.05 .

Experiment 1C [11]

The transmission of the IMS is $97 \pm 2\%$ as it should be. We measured the beam characteristics as we exercised the steering and focusing magnets. Analysis of these data is in progress. Figure 8 shows preliminary data for beam centroids, which were measured with both the emittance gear and the BPMs when we moved a steering magnet. We operated the bunchers in their accelerating and decelerating modes and found that the energy gained or lost at the design power level agreed with predictions (Fig. 9).

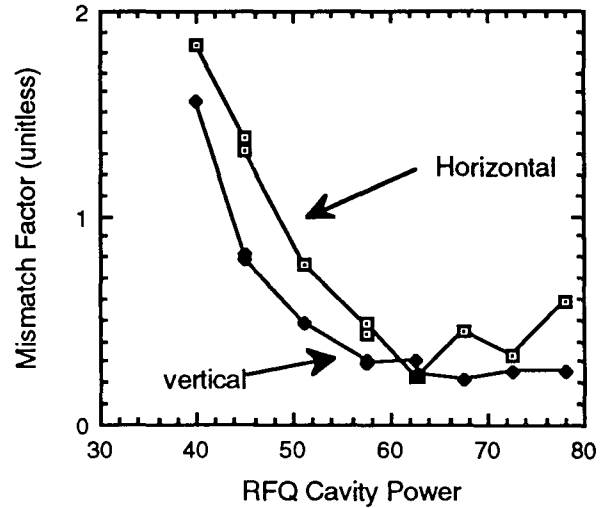


Fig. 6. Horizontal and vertical mismatch factors vs. RFQ cavity power. The minimum mismatch factor occurs between 62 and 63 kW, which is consistent with the design value.

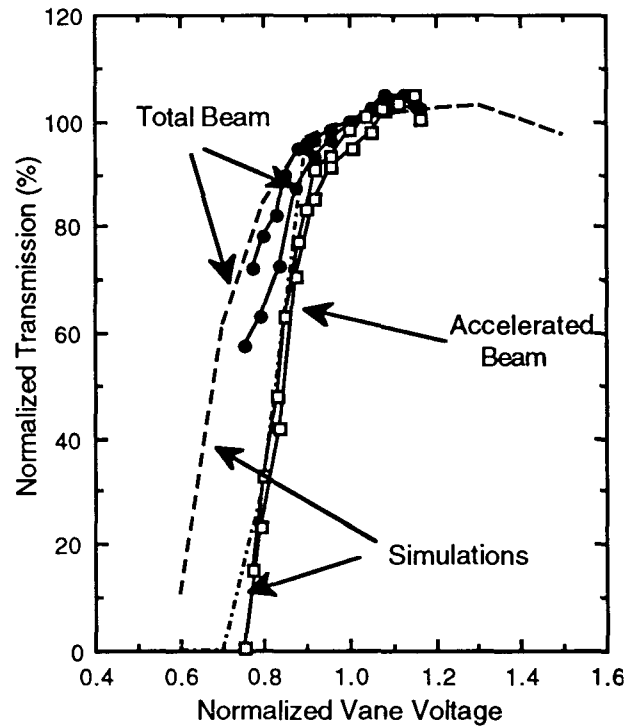


Fig. 7. Measured and simulated transmission vs. vane voltage. Data and simulations agree for a vane voltage of 56 kV and a RFQ cavity power of 62 kW.

Discussion of Results and Remaining Challenges

We find that the RFQ predicted and measured performances are in good agreement, and we find no inherent problems with running this RFQ at cryogenic temperatures. The transmission is lower than GTA specifications; however, it is consistent with simulations when actual input current and emittance areas are used and when image charge and multipole effects are included. Our

present input emittance is larger than design specifications and increases the effects of image charge and multipoles. Simulations predict that the larger emittance causes a 10% reduction in transmission and that image charge and multipole effects cause another 10% reduction. We are exploring methods of increasing the injector current and reducing its emittance.

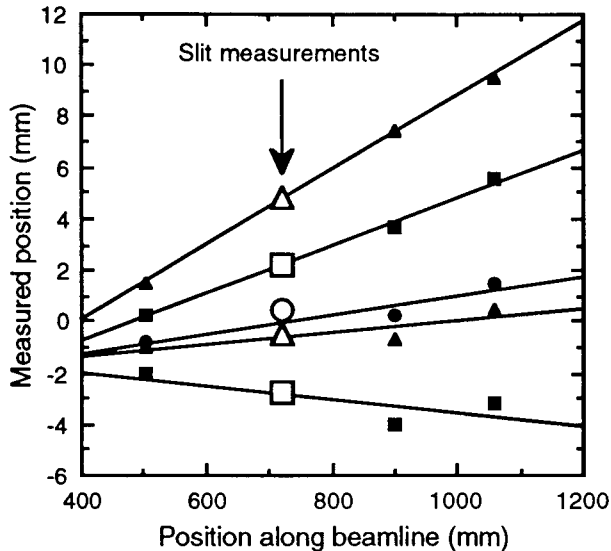


Fig. 8. Observed beam centroids vs. drift position for various IMS steering configurations. The lines are straight-line fits to the data from each configuration.

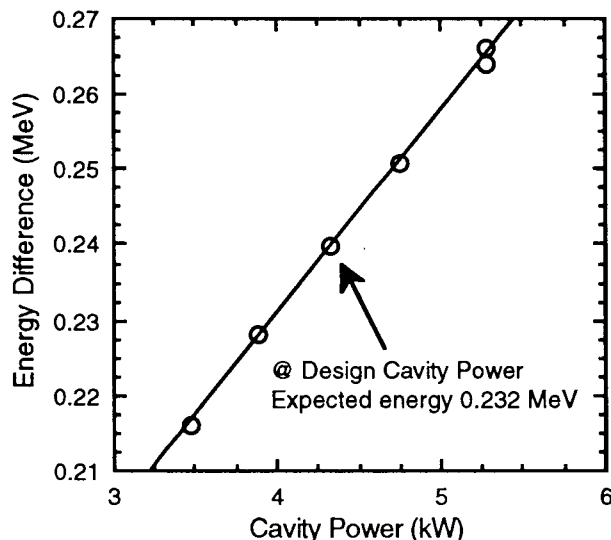


Fig. 9. Energy difference between acceleration and deceleration modes of the first IMS buncher vs. IMS cavity power. The observed energy difference agrees with predictions to within 3%.

During experiment 1C, we determined that displacement of steering magnets in either the horizontal or vertical plane caused beam displacements in the both planes. We suspect that quadrupole rotation is the cause of the coupled motion and are determining the roll angle using measured beam displacements. Later we will measure the

roll angles of all the IMS quadrupoles in situ using the taut wire method.

Our immediate plans are to continue the analysis of experiment 1C and to produce an IMS model for steering and matching the beam to the DTL. Preparation and equipment checkout is now in progress for experiment 2A, and commissioning of the first DTL module will begin in September.

Acknowledgments

Many people made important contributions in the preparation and execution of the GTA commissioning. Special thanks are due to M. Milder and the GTA facility support team for the many long hours maintaining and operating the cryo-system, the vacuum and water systems, and for the installation of the GTA components; L. Dauelsberg and the alignment team for the necessary alignment information of the beamline components and diagnostics; P. Denney and the rf team for the rf power support; M. Smith for his experimental support and his analysis efforts; and P. Prince and the assembly team for the mechanical characterization of the rf cavities.

References

1. M. Gamble, T. Thompson, and W. Miller, "Design, Analysis, and Monitoring of a Dynamic H⁰ and H⁻ Beam Sensing System," Los Alamos National Laboratory Report LA-CP-89-224 (1989).
2. W. B. Cottingham, et al., "Non interceptive Technique for the Measurement of Longitudinal Parameters of H⁻ Beams," Proc. 1985 Particle Accelerator Conference, IEEE Trans. Nucl. Sci. 32 (5), 1871 (1985).
3. R. A. Cole, "Real-Time Data Archiving for GTA," Proceedings 16th International LINAC Conference, Ottawa, Ontario, August 23-28, 1992.
4. M. W. Stettler, et al., "A Distributed Timing System for Synchronizing Control and Data Collection," Proceedings 16th International LINAC Conference, Ottawa, Ontario, August 23-28, 1992.
5. A. H. Regan, et al., "RF System Description For the Ground Test Accelerator RFQ," Proceedings 16th International LINAC Conference, Ottawa, Ontario, August 23-28, 1992.
6. C. M. Fortgang, et al., "Pulsed Taut Wire Alignment of Multiple Permanent Magnet Quadrupoles," Proceedings 1990 LINAC Conference, Albuquerque, NM, September, 1990.
7. P. Allison and J. D. Sherman, "Operating Experience with a 100-keV, 100 mA H⁻ Injector," Proceedings of the 3rd International Symposium, Brookhaven, 1983, AIP Conference Proceedings No. 111, p511
8. K. R. Crandall and D. P. Rusthoi, "TRACE 3-D Documentation," Los Alamos National Laboratory report LA-UR-90-4146 (July 1989).
9. K. F. Johnson, "Commissioning of the Ground Test Accelerator RFQ," Proceedings 16th International LINAC Conference, Ottawa, Ontario, August 23-28, 1992.
10. J. Guyard and M. Weiss, "Use of Beam Emittance Measurements in Matching Problems," Proc. 1976 Linear Accel. Conf., Atomic Energy of Canada, AECL-5677 (1976), p. 254
11. K. F. Johnson, "Commissioning the Ground Test Accelerator Intertank Matching Section," Proceedings 16th International LINAC Conference, Ottawa, Ontario, August 23-28, 1992.